Reactivity of hydroxopentaaquarhodium(III) ion towards glycine-containing dipeptides in aqueous medium

Biplab K. Bera, Arup Mandal, Parnajyoti Karmakar, Subhasis Mallick, Subala Mondal and Alak K. Ghosh*

Department of Chemistry, The University of Burdwan, Burdwan-713 104, West Bengal, India

E-mail : alakghosh2002@yahoo.co.in

Abstract : The kinetics of the interaction of two glycine-containing dipeptides, namely, glycyl-L-leucine (L^1-L'H) and glycyl-L-isoleucine (L^2-L'H) with $[Rh(H_2O)_5OH]^{2+}$ has been studied spectrophotometrically in aqueous medium as a function of $[Rh(H_2O)_5OH^{2+}]$, [dipeptide], pH and temperature at constant ionic strength. At pH 4.3, where the substrate complex and dipeptides exists predominantly as hydroxopentaaqua species and zwitter ion respectively. The reaction has been found to proceed via two parallel paths : both processes are ligand dependent. The rate constant for the processes are : $k_1 \sim 10^{-3}$ s^{-1} and $k_2 \sim 10^{-5}$ s^{-1}. The activation parameters for both the steps were evaluated using Eyring's equation. Based on the kinetic and activation parameters an associative interchange mechanism is proposed for both the interaction processes. The low $\Delta H_1^{\neq}$ and large negative value of $\Delta S_1^{\neq}$ as well as $\Delta H_2^{\neq}$ and $\Delta S_2^{\neq}$ indicate an associative mode of activation for both the aqua ligand substitution processes for both the parallel paths. The product of the reaction has been characterized, as IR and ESI-mass spectroscopic analysis.

Keywords : Kinetics, interaction, glycyl-L-leucine, glycyl-L-isoleucine, hydroxopentaaquarhodium(III) ion.

Introduction

A full understanding of the modes of action of metal based antitumoral drugs requires the study of their interactions with all possible biological targets, including amino acids, hormones, peptides and proteins. It is reasonable to expect that any injected metal drug will present some kind of interaction with these macromolecules, which could crucially determine its bioavailability and toxicology. However carcinostatic properties of platinum complexes, especially of cisplatin[1], involve special impetus to research on interaction of the metal ion with nucleic acid constituents[2-4]. Similarly, in combination with other drugs, it is effective against ovarian, small cell lung, bladder, brain and breast tumors[5]. However, it has several side-effects, and of particular importance is the renal damage which is correlated to platinum binding and inactivation of renal thiol-containing enzymes[6,7]. A large number of analogs of cisplatin have been tested and it has been reported that many active complexes could react with DNA and inhibit its synthesis[8-12]. Other transition metal complexes with favorable anti-tumor activity are gold, rhodium and palladium complexes[6,7]. The interaction of rhodium(II)
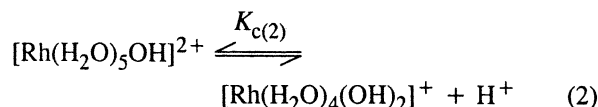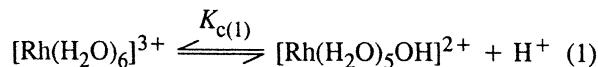
and platinum group metal antitumoral compounds with serum albumin has been reported by Esposito and Najjar[2], where rhodium is thought to react mainly through coordination with the imidazole group of histidine residues. In some earlier studies a series of antitumoral rhodium(II) carboxylates, for example, $Rh_2(CH_3CO_2)_4$, $Rh(CH_3CH_2CO_2)$, $Rh_2(CH_3CH_2CH_2CO_2)_4$ and $Rh(CF_3CO_2)_4$ were found to bind quickly to albumin[13]. Many rhodium, ruthenium, iridium and palladium complexes have also been reported to have considerable antibacterial behavior[14,15]. Rhodium and iridium complexes are also being explored for their medicinal properties as potential anticancer agents[16].

This work describes the detailed kinetic and mechanistic studies of aqua ligand substitution from hydroxopentaaquarhodium(III) ion by dipeptide which is a model dipeptide. This work is also interesting from kinetic view point showing a parallel reaction scheme.

Results and discussion

From the pK$_a$ values[17] of the dipeptides, it is clear that at pH 4.3 the major species involved in the kinetic process are the zwitterionic form of the peptides.

On the other hand the ionization of $[Rh(H_2O)_6]^{3+}$ may be given as :

$$[Rh(H_2O)_6]^{3+} \xrightleftharpoons{K_{c(1)}} [Rh(H_2O)_5OH]^{2+} + H^+ \quad (1)$$

$$[Rh(H_2O)_5OH]^{2+} \xrightleftharpoons{K_{c(2)}}$$
$$[Rh(H_2O)_4(OH)_2]^+ + H^+ \quad (2)$$

The $pK_{c(1)}$ and $pK_{c(2)}$ values of $[Rh(H_2O)_6]^{3+}$ are 3.6 and 4.7 respectively at 25 °C[18]. Other reports on the $pK_{c(1)}$ value are 3.2, 3.4 and 3.45 (references are given in 18). With increase in pH, the proportion of the more labile hydroxopentaaquarhodium(III) ion increases. The hydroxide ligand increases the water exchange rate of $[Rh(H_2O)_5OH]^{2+}$ relative to $[Rh(H_2O)_6]^{3+}$ [19]. In the studied pH range, dipeptides (L-L'H) exist mainly as the dipolar ion. As the pH increases the proportion of the more reactive anionic form increases and since the ligating capability of the deprotonated ligand is always higher than its dipolar ion form, the rate increment with rise in pH is partly accounted for. The pH range chosen in the present study is 3.0 to 4.3, where the active species involved in the reaction is L-L'H. At pH higher than 4.5, the system becomes turbid and the hydrous oxide of rhodium was precipitated quantitatively when the molar ratio of hydroxyl to rhodium, $[OH^-]/[Rh^{3+}]$, reached three[20].

At constant temperature, pH (4.3) and fixed concentration of complex (A) the $\ln (A_\infty - A_t)$ versus time (t) plot for different ligand concentration indicates a two-step process. Both are dependent on the incoming ligand concentration, and with increasing ligand concentration a limiting rate is reached. Job's method of complexation indicates a 2 : 1 metal-ligand ratio in the product complex. This is possible only when a bridged complex is formed. The rate constant for such process can be evaluated by assuming the following Scheme 1.
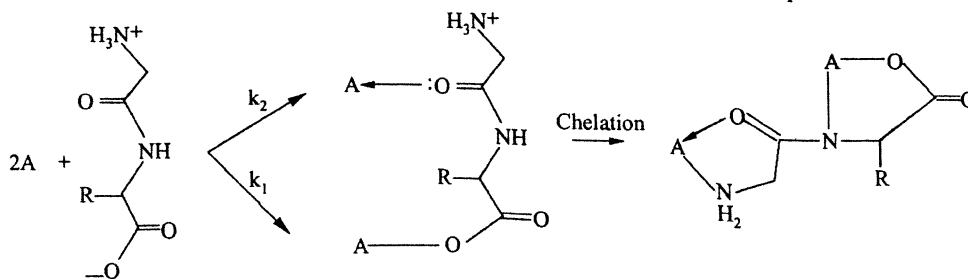
where, L, the ligand reacts to both of the Rh centres [(1) and (2)] in a parallel fashion. In the starting complex there are two equivalent rhodium(III) centers. Now the ligand has two donor centres. As rhodium(III) is a borderline centre, during the ligation two donor centres attack in two parallel speeds ($k_1 \sim 10^{-3}$ s^{-1} and $k_2 \sim 10^{-5}$ s^{-1}), which is shown in the mechanism and conclusion section.

Calculation of k_1 value for the **A** → **B** *step* :

The rate constant for the first phase of the reaction **A** → **B** was calculated from the absorbance data using the Weyh and Hamm[21] equation.

$$(A_\infty - A_t) = a_1 \exp (-k_{1(obs)} t) + a_2 \exp (-k_{2(obs)} t) \quad (3)$$

where a_1 and a_2 are constants that depend upon the rate constants and extinction coefficients.

Values of $a_2 \exp (-k_{2(obs)} t)$ at different times (when t is small) were obtained from the linear portion of the curve (Fig. 12) extended to t equals zero, i.e.

$$a_2 \exp (-k_{2(obs)} t) = (A_\infty - A_t)_{limiting}$$

Therefore values of $(A_\infty - A_t) - a_2 \exp (-k_{2(obs)} t)$ were calculated from X and Y values (Fig. 12) at different t;

$$\Delta = a_1 \exp (-k_{1(obs)} t)$$

or, $\ln \Delta = $ constant $- k_{1(obs)} t \quad (4)$

$k_{1(obs)}$ was then derived from the slope of $\ln \Delta$ versus time, when for small values of t (Fig. 13). A similar procedure was applied for each glycyl-L-leucine concentration in the 2.50×10^{-3} mol dm^{-3} to 7.50×10^{-3} mol dm^{-3} range using the experimental conditions specified in Table 1. The $k_{1(obs)}$ values are collected in Table 1.

The rate increases with increase in [L¹-L'H] and reaches a limiting value (Fig. 1). The limiting rate is probably due to the completion of outer sphere associa-

Scheme 1

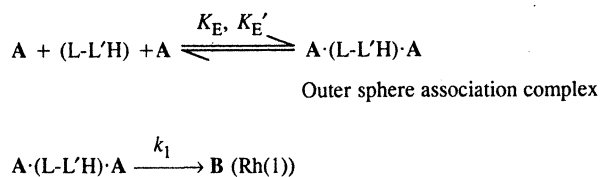**Table 1.** $10^3 k_{1(obs)}$ (s^{-1}) values for different dipeptide concentrations at different temperatures

[Complex A] = 2.5 × 10^{-4} mol dm^{-3}, pH = 4.3,
ionic strength = 0.1 mol dm^{-3} NaClO$_4$

Ligand	Temp.	10^3 [Ligand] (mol dm^{-3})				
	(±0.1 °C)	2.50	3.75	5.00	6.25	7.50
L^1-L'H	50	1.95	2.48	3.09	3.39	3.66
	55	2.15	2.90	3.36	3.68	4.18
	60	2.36	3.17	3.62	4.07	4.55
	65	2.75	3.55	4.09	4.72	5.32
L^2-L'H	50	2.09	2.78	3.15	3.56	4.03
	55	2.47	3.14	3.78	4.17	4.57
	60	2.75	3.56	4.10	4.64	5.06
	65	3.25	4.20	4.78	5.46	5.78
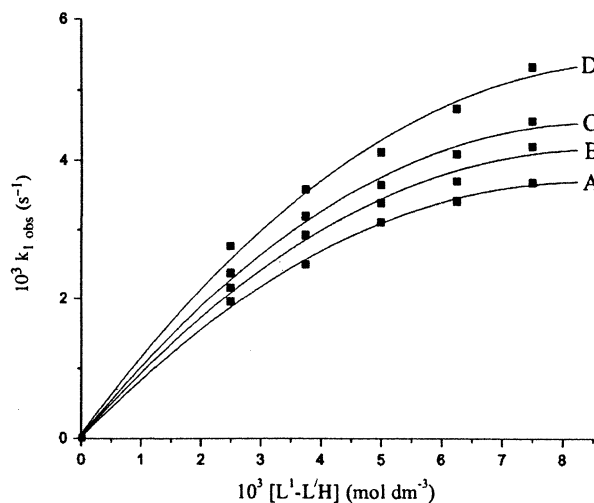
Fig. 1. Plot of $k_{1(obs)}$ versus [L^1-L'H] at different temperature, A = 50, B = 55, C = 60 and D = 65 °C.

tion complex formation. Since the metal ion reacts with its immediate environment, further change in [L^1-L'H] beyond the saturation point will not affect the reaction rate. The outer sphere association complex may be stabilized through H-bonding[22,23].

Based on the experimental findings, the following Scheme 2 may be proposed for the step **A → B**;

$$A + (L-L'H) + A \underset{K_E, K_E'}{\overset{}{\rightleftharpoons}} A \cdot (L-L'H) \cdot A$$

Outer sphere association complex

$$A \cdot (L-L'H) \cdot A \xrightarrow{k_1} B \ (Rh(1))$$

Scheme 2

Based on the above scheme a rate expression can be derived for the **A → B** step

$$d[B]/dt = k_1 K_E [Rh(H_2O)_5(OH)^{2+}]^2[\text{dipeptide}] \quad (5)$$

or,

$$d[B]/dt = k_{1(obs)}[Rh(H_2O)_5(OH)^{2+}]^2_T \quad (6)$$

where T stands for total concentration of Rh^{III}. We can then write,

$$k_{1(obs)} = k_1 K_E [L-L'H]/(1 + K_E [\text{dipeptide}]) \quad (7)$$

where k_1 is the rate constant for the **A → B** step, i.e. the rate constant for the interchange of outer sphere complex to the inner sphere complex; K_E is the outer sphere association equilibrium constant.

The equation can be represented as :

$$1/k_{1(obs)} = 1/k_1 + 1/k_1 K_E [\text{dipeptide}] \quad (8)$$

The plot of $1/k_{1(obs)}$ against $1/[\text{dipeptide}]$ should be linear with an intercept of $1/k_1$ and slope $1/k_1 K_E$. This was found to be the case at all temperatures studied. The k_1 and K_E values were calculated from the intercept and slope (Fig. 2) and are collected in Table 3.
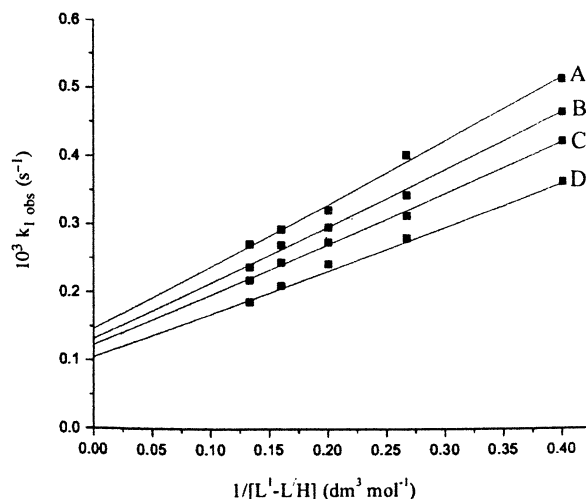
Fig. 2. Plot of $1/k_{1(obs)}$ against $1/[$ L^1-L'H], A = 50, B = 55, C = 60 and D = 65 °C.

The rate constants for this step were calculated from the latter linear portions of the graphs and are collected in Table 2. This is again dependent on [dipeptide] and shows a limiting value at higher ligand concentrations (Fig. 2). The coordinated dipeptide at any of the rhodium(III) centres now attacks the second rhodium(III) centre. The intermediate here is also possibly stable

451

Table 2. $10^5 k_{2(obs)}$ values for different dipeptide concentrations at different temperatures

[Complex A] = 2.5 × 10^{-4} mol dm^{-3}, pH = 4.3, ionic strength = 0.1 mol dm^{-3} $NaClO_4$

Ligand	Temp.	10^3 [Ligand] (mol dm^{-3})				
	(±0.1 °C)	2.50	3.75	5.00	6.25	7.50
L^1-L'H	50	2.04	2.60	2.94	3.36	3.55
	55	3.98	4.90	5.68	6.17	6.49
	60	7.58	9.09	10.31	10.99	11.89
	65	12.50	14.71	17.24	18.18	18.87
L^2-L'H	50	2.19	2.75	3.16	3.58	3.77
	55	3.89	4.78	5.56	6.09	6.67
	60	7.25	9.09	9.89	10.64	11.76
	65	13.16	15.15	17.54	18.87	19.61

Table 3. The k_1, k_2, K_E and K'_E values for different dipeptide at different temperatures

[Complex A] = 2.5 × 10^{-4} mol dm^{-3}, pH = 4.3, ionic strength = 0.1 mol dm^{-3} $NaClO_4$

Ligand	Temp.	$10^3 k_1$	K_E	$10^5 k_2$	K'_E
	(±0.1 °C)	(s^{-1})	(dm^3 mol^{-1})	(s^{-1})	(dm^3 mol^{-1})
L^1-L'H	50	6.71	162	5.65	225
	55	7.47	164	9.63	282
	60	8.11	166	15.67	327
	65	9.24	168	25.92	368
L^2-L'H	50	7.03	170	5.98	290
	55	7.84	183	10.02	323
	60	8.51	191	16.23	368
	65	9.58	206	26.17	395

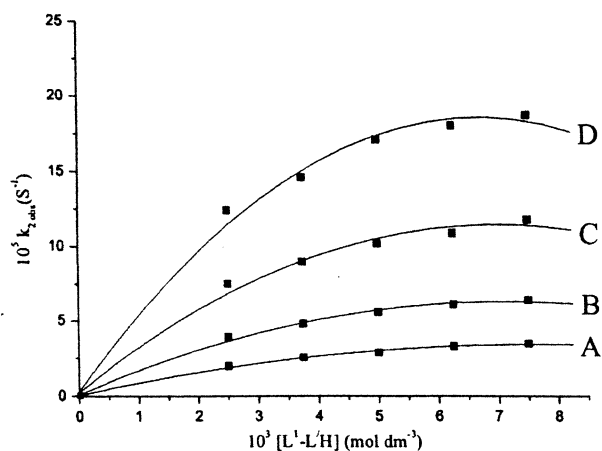**Fig. 3.** Plot of $k_{2\ (obs)}$ versus [L^1-L'H] at different temperature, A = 50, B = 55, C = 60 and D = 65 °C.
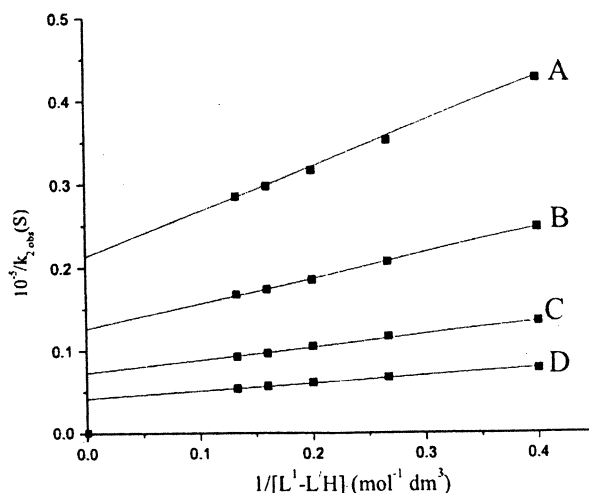

Fig. 4. Plot of $1/k_{2(obs)}$ against $1/$[L^1-L'H], A = 50 , B = 55, C = 60 and D = 65 °C.

through H-bonding between coordinated water and the approaching dipeptide dipolar ion. When two paths are parallel, then two rates are overlapping. When we are calculating the k_1 ($\sim 10^{-3}$ s^{-1}), the contribution from k_2 (10^{-5} s^{-1}) is negligible; once again when we are calculating k_2, the k_1 path is already completed. Thus there is no problem in calculating both the rate constants.

The k_2 and K'_E for the **A** → **B** step is calculated in a manner similar to eq. (8) (Fig. 4) and data are collected in Table 3.

Based on the experimental findings, a two step interchange associative mechanism is proposed for the substitution process for both the paths. In the first step, an outer-sphere association complex is formed between the ligand and the two rhodium(III) centers, which is stabilized by the H-bonding between the incoming dipeptide

and the coordinated aqua molecules. Now the interchange of the ligand from the outer-sphere to the inner-sphere occurs. Both paths of the final phase of substitution reaction are the chelation step to give the product complex which is independent of dipeptide concentration.

Effect of pH on the reaction rate :

The reaction was studied at five different pH values (3.0, 3.3, 3.6, 4.0 and 4.3). The $k_{1(obs)}$ and $k_{2(obs)}$ values increased with increase in pH; at fixed concentration of (2.5 × 10^{-4} mol dm^{-3} of [complex A], 7.50 × 10^{-3} mol dm^{-3} [L^1-L'H]) and 0.1 mol dm^{-3} ionic strength, the 10^3 $k_{1(obs)}$ values at 60 °C were 1.89, 2.18, 3.02, 3.97 and 4.55 s^{-1} and 10^5 k_2 values were 3.99, 7.28, 9.32, 11.11 and 11.89 s^{-1} at 3.0, 3.3, 3.6, 4.0 and 4.3 respectively. The enhancement in rate may be explained based on the acid dissociation equilibria of the reactants. A rate ex-

pression for path 1 may be given :

$$k_{obs} = \frac{k_1\, K_E\, K_{c(1)}\, K_a\, [\text{dipeptide}]_t}{K_a\, K_{c(1)}\, (1\, +\, K_E\, [\text{dipeptide}]_t)\, +}$$
$$[\text{H}^+]\, (K_a\, +\, K_{c(1)})\, +\, [\text{H}^+]^2$$

where k_1 and K_E are rate constant and outer-sphere association equilibrium constant and also $K_{c(1)}$ and K_a are acid dissociation constants of $[\text{Rh}(\text{H}_2\text{O})_6]^{3+}$ and for the ligand COOH.

Further study of the substitution reaction was followed at pH 4.3 to avoid complications caused by adding an additional parameter $[\text{H}^+]$ to the rate equation. At pH 4.3, the complex exists mainly in the hydroxopentaaqua form and the contribution due to the hexaaqua species is negligible. With increasing pH the complex also changes its form from aqua to hydroxoaqua and the hydroxide ligand increases the water exchange rate constant of $[\text{Rh}(\text{H}_2\text{O})_5(\text{OH})]^{2+}$ relative to $[\text{Rh}(\text{H}_2\text{O})_6]^{3+}$. However, the dipeptide acts as a buffer during the reaction.

Effect of temperature :

The reaction was studied at four different temperatures for different ligand concentrations and the results are listed in Tables 1 and 2. The two rate constants k_1 and k_2 are sensitive to changes of temperature. The activation parameters for both the steps $\text{A} \xrightarrow{k_1} \text{Rh}^1(\text{B})$ and $\text{A} \xrightarrow{k_2} \text{Rh}^2(\text{B})$ were evaluated from the linear Eyring plots (Figs. 5 and 6). The activation parameters were collected in Table 4.

Fig. 5. Eyring plot for k_1.

Fig. 6. Eyring plot for k_2.

Table 4. Activation parameters for [complex A] by dipeptides in aqueous medium, pH = 4.3

Ligands	$\Delta H_1^{\neq}$ (kJ mol^{-1})	$\Delta S_1^{\neq}$ (JK^{-1} mol^{-1})	$\Delta H_2^{\neq}$ (kJ mol^{-1})	$\Delta S_2^{\neq}$ (JK^{-1} mol^{-1})
L^1-L'H	16.4 ± 0.7	–236 ± 2	87.5 ± 0.9	–56 ± 3
L^2-L'H	15.3 ± 0.8	–239 ± 2	84.9 ± 1.1	–63 ± 3

The low $\Delta H^{\neq}$ values are in support of the ligand participation in the transition state for both the steps. The high negative $\Delta S^{\neq}$ values suggest a more compact transition state, where both the incoming and departing ligands are attached in the transition state, and this is also in support of the assumption of a ligand participated transition state.

Mechanism and conclusion :

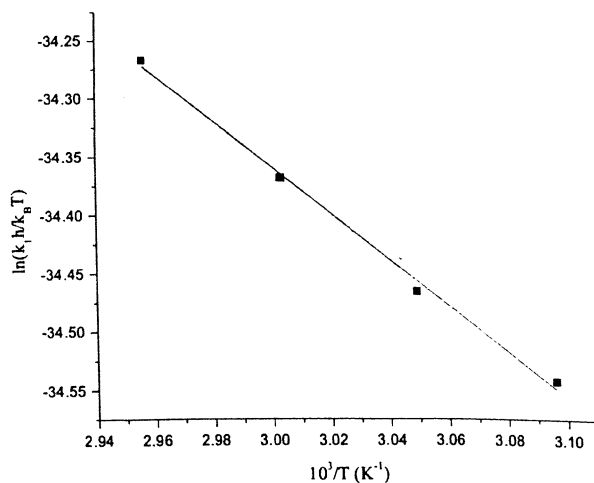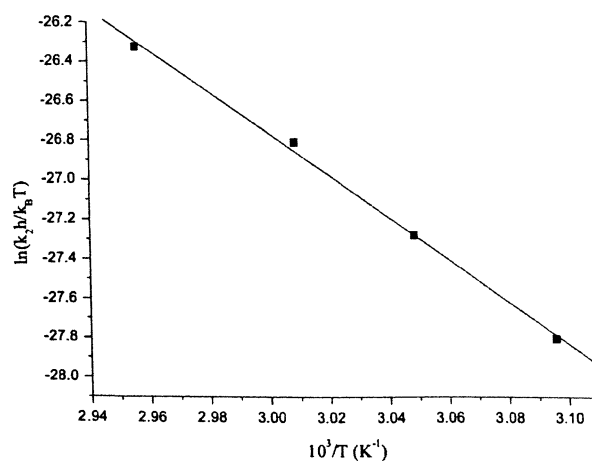Each dipeptide has one carboxyl group and one amino group at the opposite ends of the molecule. Because of neutrality of the amide group, the two terminal groups are the most effective bonding sites for metal coordination but steric requirements preclude the simultaneous coordination of three groups to the same metal ion. Also tetra coordination complex formation may be possible when two metal ions are participated.

The complex of dipeptides such as glycyl-glycine with various metal ions has been studied. The metal ions, which are able to promote amide deprotonation, are the most interesting in this field. A literature survey[24] shows that Pd^{II}, Cu^{II} and Ni^{II} are most effective in this respect. There are reports of Fe^{II} and Fe^{III} induced deprotonation of the amide groups[25,26].

Dipeptide may coordinate to Rh^{III} ion in four ways.

(i) Monodentate coordination through carboxylate-O to give 1 : 1 and 1 : 2 products.

(ii) Bidentate coordination involving amino-N and carbonyl-O is expected to occur at low pH where amide deportation is difficult[27].

(iii) Tridentate coordination involving terminal carboxylate-O, amide-N, and amino-N groups gives rise to two fused five-membered rings. This has been observed with Cu^{II}, Pd^{II} and Ni^{II} complexes[26] in slightly alkaline medium.

(iv) Tetradentate coordination involving amino-N, carbonyl-O, peptide-N, and carboxylate-O gives a 2 : 1 (metal : ligand) five-membered chelated product of high stability[28]. This type of chelation occur[29] at and above pH 4.

As the substrate is a hydroxopentaaqua complex at experimental pH 4.3 and Job's method confirms the formation of a 2 : 1 chelate product, so the first three possibilities are ruled out. At first the dipeptide binds to the rhodium center through carboxylate-O^- and peptide-O which shows high affinity for Rh^{III}, a borderline acid. The carboxylate-O^- has more electron density and so it react faster rate than other.

The interaction of dipeptide with the titled rhodium complex proceeds via two distinct parallel substitution steps of aqua molecules ($k_1 \sim 10^{-3}$ s^{-1} and $k_2 \sim 10^{-5}$ s^{-1}). Each step proceeds via an associative interchange activation. At the outset of each step outer sphere association complex results, which is stabilised through H-bonding and is followed by an interchange from the outer sphere to the inner sphere complex. The outer sphere association equilibrium constants, a measure of the extent of H-bonding for each step at different temperatures are evaluated (Table 3). The activation parameters values for both the steps suggest an associative mode of activation for the substitution process. The $\Delta H_1^{\neq}$ and $\Delta H_2^{\neq}$ values and negative $\Delta S_1^{\neq}$ and $\Delta S_2^{\neq}$ values imply a good degree of ligand participation in the transition state.

From a comparison of the dipeptides used, it can be concluded that the variation in size and bulkiness of the entering dipeptides reflects their properties as nucleophiles. The differences in reactivity of the selected dipeptides is obvious and their reactivity follows the order L^1-L'H <

L^2-L'H. The sensitivity of the reaction rate towards the donor properties of the entering ligands is in the line with that expected for an associative mode of activation. In addition, donor effects (present in different R group of dipeptide) are more important than steric effect due to the presence of water molecules in the hydroxopentaaquarhodium complexes. Also the entering dipeptide was stabilized by hydrogen bonding with water molecule of hydroxopentaaquarhodium complexes. For the two dipeptides increasing donor affects reactivity increases which reflects in their rate constants values. Also from ESI-MS measurement a chelated product in the final step is proposed.

Based on the above facts, a plausible mechanism for the substitution has been proposed as shown in the following (Fig. 7).

Experimental

[Rh(H$_2$O)$_6$](ClO$_4$)$_3$ was prepared as per literature method[30] and characterized by chemical analysis and spectroscopic data[31] ($\lambda_{max} = 396$ nm, $\varepsilon = 62$ dm^3 mol^{-1} cm^{-1}; $\lambda_{max} = 311$ nm, $\varepsilon = 67.4$ dm^3 mol^{-1} cm^{-1}). The reactant complex [Rh(H$_2$O)$_5$(OH)](ClO$_4$)$_2$ (complex A) was obtained in situ (yield ~90%) by adjusting the pH to 4.3. Higher proportions of complex could not be obtained as the solution becomes turbid at higher pH. The reaction product of dipeptides (7.5 × 10^{-3} mol dm^{-3}) and complex A (2.5 × 10^{-4} mol dm^{-3}) were (substituted complex; complex C and complex D) prepared by mixing the reactants in different ratios namely 1 : 1, 1 : 2, 1 : 3, 1 : 5 and 1 : 10, and equilibrating the mixtures at 60 ± 0.1 °C for 72 h. The absorption spectra of these mixtures (Fig. 8) all exhibited the same λ_{max} (230 nm) with nearly identical intensities. The composition of the product in the reaction mixture was determined by Job's method of continuous variation (Fig. 9). The metal-ligand ratio was found to be 2 : 1. Doubly distilled water was used to prepare all the kinetic solutions. The ligand dipeptides were obtained from HIMEDIA. All chemicals used were of AR grade available commercially. The reactions were carried out at constant ionic strength (0.1 M NaClO$_4$). Complex A and the ligand were mixed in 2 : 1 molar ratio in a reaction vessel and heated at 60 °C for 72 h, then transferred in a glass beaker and slowly evaporated
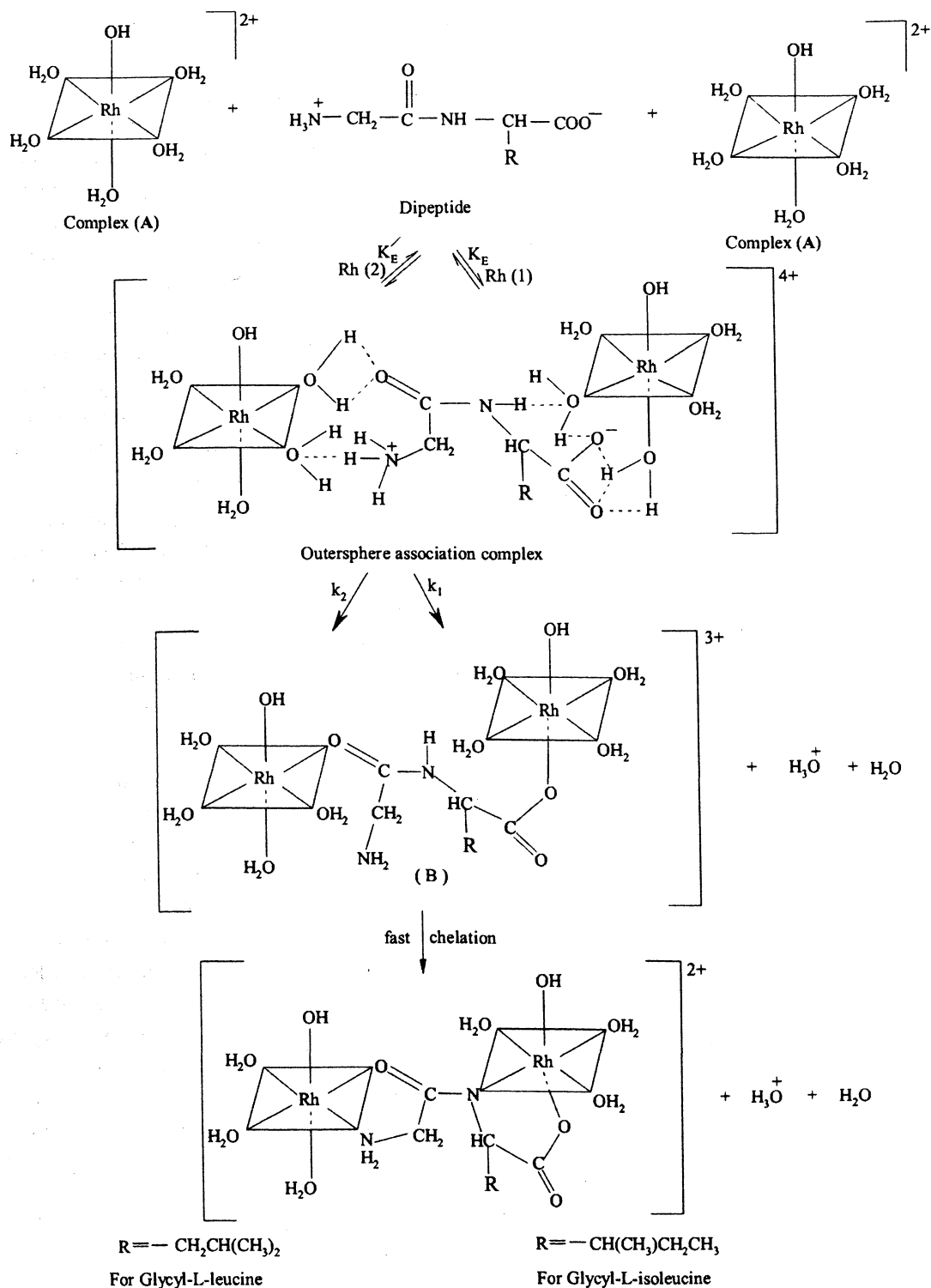
Fig. 7. Proposed mechanism for the interaction of dipeptide with the complex A.

at room temperature and finally in a desiccators. This product was used for IR and ESI-mass spectroscopic analysis.

We have characterized the product by IR and MS spectrometric analysis which also substantiate our study.
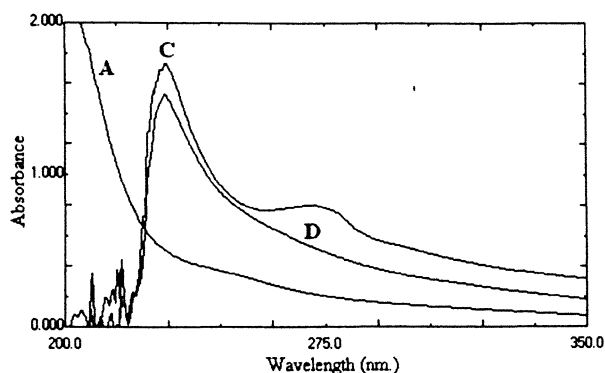
455

Fig. 8. Spectra of the starting complex (**A**), glycyl-L-leucine (L¹-L′H) substituted complex (**C**), glycyl-L-isoleucine (L²-L′H) substituted complex (**D**); [Complex **A**] = 2.5 × 10⁻⁴ mol dm⁻³, [dipeptide] = 7.5 × 10⁻³ mol dm⁻³, pH = 4.3, cell used = 1 cm quartz.
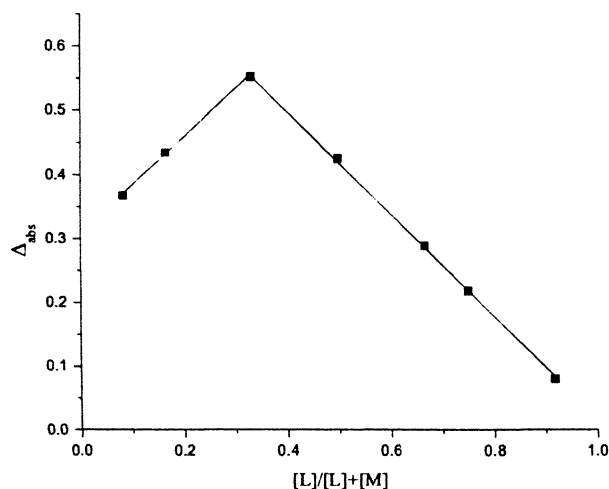

Fig. 9. Job's plot for reaction of complex **A** with glycyl-L-leucine.

$[Rh(H_2O)_5(OH)]^{2+}$ and glycine-L-leucine (L¹-L′H) were mixed in 2 : 1 molar ratio at pH 4.3 and a pale yellow product was obtained. The IR spectra of the pale yellow product in the KBr disc show strong bands in the region ~3439–3071 cm⁻¹ together with medium bands at 1626, 535 and 402 cm⁻¹. The asymmetric COO⁻ stretching frequency (v_{asym}) of the amino acids occurs at 1580–1660 cm⁻¹ when the group is coordinated to metals, where as a non-coordinated COO⁻ group has the v_{asym} (COO⁻) stretching at lower frequency[32]. The band at 1626 cm⁻¹ is therefore due to the v_{asym} (COO⁻) of the metal bounded carboxyl group. The band at ~3244–3071 cm⁻¹ indicates NH stretching frequency. The presence of strong stretching band at ~3439 cm⁻¹ indicates that product contains

aqua or hydroxyl ligands. The bands at 535 and 402 cm⁻¹ are assigned to v(Rh–N) and v(Rh–O) bond formation respectively[33]. An intense band of the v(C=O)$_{amide}$ at 1691 cm⁻¹ in the non-coordinated glycine-L-leucine undergoes a bathochromic of ~65 cm⁻¹ shift in the IR spectra upon complexation. This is probably due to the involvement of the peptide nitrogen (because of the deprotonation that has taken place) in bonding with Rh^{III}, which lowers the bond order of the v(C=O)$_{amide}$ group due to resonance stabilization.

The aqueous solution of $[Rh(H_2O)_5(OH)]^{2+}$ and glycyl-L-leucine were mixed in a 2 : 1 molar ratio and the mixture was thermostated at 60 °C for 48 h and used for ESI-MS measurement. The ESI mass spectra of the resulting solution are shown in Fig. 10.

It is clear from this spectrum that the ion at *m/z* 303.0249 (minor peak) has become the precursor ion species in the mixture solution and this is tentatively attributed to (glycyl-L-leucine + $2Rh^{3+}$ + $10H_2O$ + $2HO^-$)$^{2+}$. Such a structure may be stabilized through the H-bonding between coordinated water molecules and solvent water molecules. The precursor ion is shown in Fig. 11.

Physical measurements :

All the spectra and kinetic measurements were recorded with a Shimadzu UV-Vis spectrophotometer (UV-1601 PC), attached to a thermoelectric cell temperature controller (model TCC-240A with an accuracy of ±0.1 °C). IR Spectra (KBr disc, 4000–300 cm⁻¹) were measured with a Perkin-Elmer FTIR model RX1 Infrared spectrophotometer. ESI-mass spectra recorded using a micromass Q-T of micro™ mass spectrometer in +ve ion mode. The pHs of the solutions were adjusted with HClO₄/NaOH and measured with a Sartorius pH meter (model PB11) with an accuracy of ±0.01. We did not add any buffer as the dipeptide in its zwitterionic form acts as a buffer.

Kinetic studies :

The progress of the reaction was monitored by the absorbance measurements at different intervals of time with a Shimadzu spectrophotometer (UV-1601 PC) attached to a thermoelectric cell temperature controller (TCC-240A). The development of a characteristic peak of the product complex (complex **C** and complex **D**) at 230 nm was monitored with time at different fixed tem-
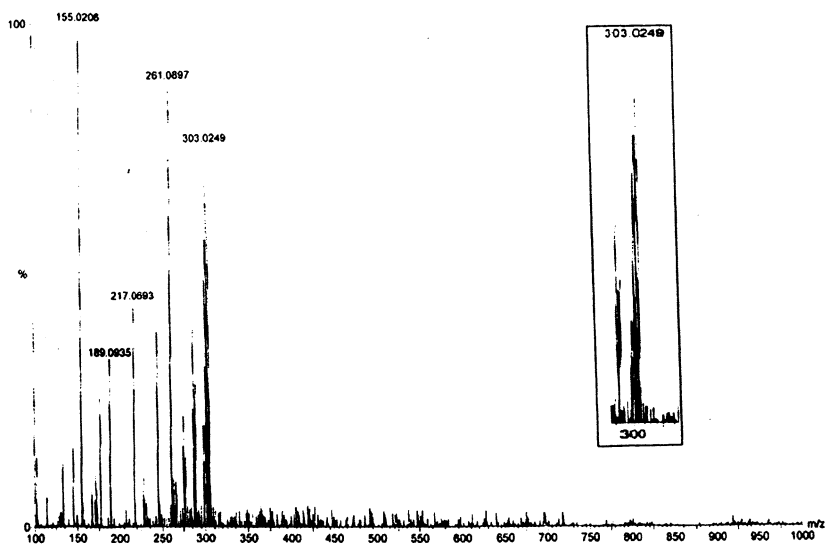
Fig. 10. ESI-mass spectra of the product of complex A with glycyl-L-leucine.
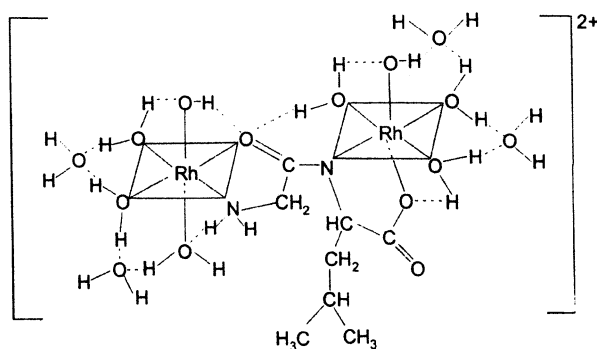

Fig. 11. Plausible structure of the precursor ion peak from the ESI-mass spectra.

peratures. The conventional mixing technique was followed and a pseudo-first order conditions were employed throughout.

The plot of ln $(A_\infty - A_t)$ (where A_t and A_∞ are absorbance at time t and after completion of reaction) against time (Fig. 12) were found to be nonlinear; being curved at the initial stage and subsequently linear in nature indicating that the reaction proceeds via two steps mechanism. From the limiting linear portion of the curve, the values of $k_{2(obs)}$ was obtained. The $k_{1(obs)}$ values were obtained from the slope of ln Δ versus time when t is small (Fig. 13). Where D is the difference of $(A_\infty - A_t)$ values between the measured and extrapolated part of the linear portion of ln $(A_\infty - A_t)$ versus time (t) curve at any time (t). The reported rate data represented as an average of duplicate runs were reproducible to within $\pm 4\%$.
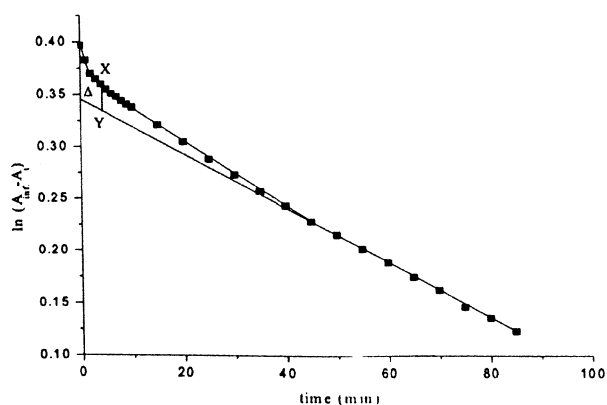

Fig. 12. A plot of ln $(A_\infty - A_t)$ versus time. [Complex A] = 2.5 × 10^{-4} mol dm^{-3}, [L^1-L'H] = 7.5 × 10^{-3} mol dm^{-3}, pH = 4.3, ionic strength = 0.1 mol dm^{-3} NaClO$_4$.

Fig. 13. Plot of ln Δ versus time. [Complex A] = 2.5 × 10^{-4} mol dm^{-3}, [L^1-L'H] = 7.5 × 10^{-3} mol dm^{-3}, pH = 4.3, ionic strength = 0.1 mol dm^{-3} NaClO$_4$.
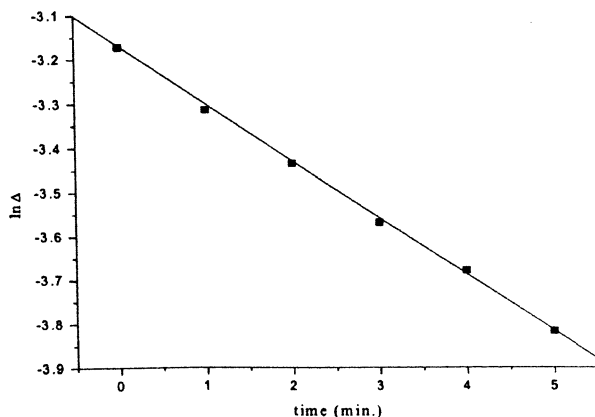
457

References

1. B. Rosenberg, L. Vancamp and T. Krigas, *Nature (London)*,1965, **205**, 698.

2. B. P. Esposito and R. Najjar, *Coord. Chem. Rev.*, 2002, **232**, 137.

3. D. Banerjea, T. A. Kaden and H. Sigel, *Inorg. Chem.*, 1981, **20**, 2586.

4. P. Umapathy, *Coord. Chem. Rev.*, 1989, **95**, 129.

5. B. Desoize and C. Madoulet, *Crit. Rev. Oncol. Hematol.*, 2002, **42**, 317.

6. "Metallotherapeutic Drugs and Metal-based Diagnostic Agents", eds. M. Gielen and E. R. T. Tiekink, Wiley, 2004.

7. "Platinum and Other heavy Metal Compounds in Cancer Chemotherapy : Molecular Mechanism and Clinical Applications", Bonetti, Leone, Muggia and Howell, 2008.

8. A. Divsalar, A. A. Saboury, H. Mansouri-Torshizi and A. A. Moosavi-Movahedi, *J. Biomol. Struct. Dyn.*, 2007, **25**.

9. Z. Guo and P. J. Sadler, *Adv. Inorg. Chem.*, 2000, **49**, 183.

10. A. Divsalar, A. A. Saboury, R. Yousefi, A. A. Moosavi-Movahedi and H. Mansouri-Torshizi, *Int. J. Biol. Macro.*, 2007, **40**, 381.

11. H. Mansouri-Torshizi, S. Ghadimy and N. Akbarzadeh, *Chem. Pharm. Bull.*, 2001, **49**, 1517.

12. H. Mansouri-Torshizi, M. Islami-Moghaddam and A. A. Saboury, *Acta Biochimica et Biophysica Sinica*, 2003, **35**, 886.

13. B. P. Esposito, E. Oliveira, S. B. Zyngier and R. Najjar, *J. Braz. Chem. Soc.*, 2000, **11**, 447.

14. M. J. Clarke, in "Inorganic Chemistry in Biology and Medicine", ed. A. E. Martell, ACS Symp. Series 140, American Chemical Society, Washington DC, 1980, p 157 and references cited therein.

15. P. F. Pruchink, M. Bien, T. Lachowicz and Tadeusz, *Met. Based Drugs,* 1996, **4**, 185.

16. (a) M. A. Scharwitz, I. Ott, Y. Geldmacher, R. Gust and W. S. Sheldrick, *J. Organomet. Chem.*, 2008, **693**, 2299; (b) A. Dorcier, W. H. Ang, S. Bolao, L. Gonsalvi, L. Juillerat-Jeannerat, G. Aurenczy, M. Peruzzini, A. D. Phillips, F. Zanobini and P. Dyson, *J. Organometallics,* 2006, **25**, 4090.

17. A. E. Martell and R. M. Smith, "Critical Stability Constants", Vol. I, 'Amino Acids', Plenum Press, New York, 1974, 299.

18. I. Banyai, J. Glaser, M. C. Read and M. Sandstroem, *Inorg. Chem.,* 1995, **34**, 2423.

19. A. Patel, P. Leitch and D. T. Richens, *J. Chem. Soc., Dalton Trans.*, 1991, 1029.

20. J. S. Forrester and G. H. Ayres, *J. Phys. Chem.*, 1959, **63**, 1979.

21. J. A. Weyh and R. E. Hamm, *Inorg. Chem.*, 1969, **8**, 2298.

22. G. A. Jeffrey, "An Introduction to Hydrogen Bonding", University Press, Oxford, 1997.

23. G. R. Desiraju and T. Steiner, "The Weak Hydrogen Bonding in Structural Chemistry and Biology", Oxford University Press, Oxford, 1999.

24. K. Burger, "Biocoordination Chemistry; Coordination Equilibria in Biologically Active Systems", Ellis Horwood Limited, Chichester, West Sussex, PO191ED, England, 1996.

25. R. J. Motekaitis and A. E. Martell, *J. Am. Chem. Soc.*, 1970, **92**, 4222.

26. A. M. Bowles, W. A. Szarek and M. C. Baird, *Inorg. Nucl. Chem. Lett.*, 1971, **7**, 25.

27. A. M. Goswami and K. De, *Transition Met. Chem.*, 2007, **32**, 422.

28. D. A. Buckingham, C. E. Davis, D. M. Foster and A. M. Sargeson, *J. Am. chem. Soc.,* 1970, **92**, 5571.

29. T. G. Appleton, J. R. Hall, T. W. Hambley and P. D. Prenzler, *Inorg. Chem.*, 1990, **29**, 3562.

30. G. H. Ayres and J. S. Forrester, *J. Inorg. Nucl. Chem.*, 1957, **3**, 365.

31. W. C. Wolsey, C. A. Reynolds and J. Kleinberg, *Inorg. Chem.*, 1963, **2**, 463.

32. G. Pneumatikakis and N. Hadjiliadis, *J. Inorg Nucl. Chem.*, 1979, **41**, 429.

33. D. Steel and P. F. M. Verhoeven, *Vibrational Spectroscopy*, 2001, **25**, 29.